GAS SENSORS BASED ON DIAMOND HETEROSTRUCTURES FOR AIR QUALITY MONITORING

[1,2]Michal KOČÍ, [1]Ondrej SZABÓ, [3]Tibor IZSÁK, [3]Michaela SOJKOVÁ, [4]Marcin GODZIERZ, [4]Paweł WRÓBEL, [2]Miroslav HUSÁK, [1]Alexander KROMKA

[1]Institute of Physics of the Czech Academy of Sciences, Prague, Czech Republic, EU, kocim@fzu.cz

[2]Faculty of Electrical Engineering, Czech Technical University in Prague, Czech Republic, EU

[3]Institute of Electrical Engineering, Slovak Academy of Sciences, Bratislava, Slovak Republic, EU

[4]Centre of Polymer and Carbon Materials of the Polish Academy of Sciences, Zabrze, Poland, EU

https://doi.org/10.37904/nanocon.2023.4785

Abstract

Currently, great emphasis is placed on air quality and the presence of pollutants, whether on toxic substances (NH_3 or CO), substances that reduce the quality of life (CO_2) or chemical vapors from industries (acetone or ethanol). Attention is therefore focused on new gas-sensing materials enabling detection even at low (up to room) temperatures with sufficient response and short reaction time.

Here, we investigate the suitability of hydrogen-terminated nanocrystalline diamond (H-NCD) films and their heterostructures with molybdenum disulfide (MoS_2), graphene oxide (GO), reduced GO (rGO), thiol-functionalized GO (SH-GO), or gold nanoparticles (Au NPs) for gas sensing applications. Electrical properties are measured for oxidizing gas NO_2, reducing gas NH_3, and chemical vapor of ethanol (C_2H_5OH), and at temperatures varied from room temperature to 125 °C. All tested gases were used with a concentration of up to 100 ppm. Synthetic air is used as the flushing gas. The measured parameters of the tested sensors are compared, both with each other and with commercial sensors, and subsequently evaluated. In contrast to the individual forms of employed materials with limited response to the exposed gases, the H-NCD heterostructures revealed better sensing properties. In particular, the Au NPs/H-NCD heterostructures revealed a higher response at 125 °C in contrast to H-NCD, MoS_2/H-NCD had quite good response even at room temperature and GO/H-NCD revealed high sensitivity to chemical vapor, which further improved for the SH-GO/H-NCD.

Keywords: Gas sensors, nanocrystalline diamond, heterostructures, air quality monitoring

1. INTRODUCTION

Air quality is essential, especially regarding hazardous substances like ammonia (NH_3), as well as those that reduce our overall quality of life, such as nitrogen dioxide (NO_2) or carbon oxide (CO_2). The release of an increasing number of harmful substances into the air, mainly by industry, significantly threatens the quality of our lives. Nowadays, air quality monitoring and pollutant detection are significant issues. As a result, gas sensors have become almost indispensable parts of industrial processes and everyday life. Currently, the most used gas sensor that uses the conductivity principle is metal oxide (MO_X) material, especially SnO_2 [1,2]. MO_X sensors are used for their low price and flexible production. On the other hand, these sensors need a very high operating temperature, and the dimensions cannot be reduced too much [3,4]. The high energy consumption and large dimensions prevent applications as sensor nodes in IoT (Internet of Things) applications with Energy Harvesting supply. Therefore, developing devices that work at room temperature (about 22 °C) with low cost and high sensitivity is still challenging. For this reason, high demands are placed on developing new types of

sensors [1,2]. With new materials and processing, smaller, more accurate, and cheaper sensors with lower power consumption are being developed. Following that, great attention is focused on new materials suitable for gas sensors. Gas sensors with wide bandgap semiconductors (exceptionally diamond-thin layers) [5,6,7] or 2D materials (e.g., TMDs [8,9,10] or GOs [11,12]) active layers have great potential due to possible miniaturization and modification, e.g., material science or technology progress [2]. Here, a miniaturized conductivity gas sensor is realized with H-NCD films and their heterostructures with MoS_2, GOs (GO, rGO, and SH-GO), and Au NPs, which revealed enhanced gas-sensing parameters.

2. EXPERIMENTAL

The fabrication of active layers for gas sensors (pure materials and heterostructures) is described in the following chapters. The glass substrate with an interdigital (IDT) structure from Micrux was used instead of MoS_2 layers, which were prepared on Si substrate. The IDT structure from Micrux contains 90 pairs of 10 µm width gold electrodes with 200 nm thickness and 10 µm gap between electrodes. The Au/Ti IDT structures with a 120 nm thick were evaporated on the top of MoS_2 layers. Then, the substrates were ultrasonically cleaned in acetone, subsequently in isopropyl alcohol, and finally in deionized water for 10 minutes. All fabricated sensors, the distinct materials and their heterostructures are depicted in the **Figure 1**.

2.1 H-NCD

The H-NCD layers were grown by microwave plasma-enhanced chemical vapor deposition (MW-PECVD) technology. A four-step process was used: 1) preparation of a diamond nucleation layer on the substrate by treatment in an ultrasonic bath in a water-based nanodiamond powder suspension, 2) growth of the adhesion NCD layer in a linear antenna MW-PECVD system consisting of two linear antennas for better adhesion between the substrate and functional NCD layer, 3) growth of the functional NCD layer in a focused MW-PECVD chamber, and 4) surface functionalization of the NCD layer by hydrogen termination (H-NCD) realized in hydrogen plasma [13].

2.2 MoS_2

The MoS_2 layers were prepared as follows. Firstly, a 4 nm thin Mo layer was deposited using DC magnetron sputtering in an Ar atmosphere from a Mo target at room temperature (about 22 °C). The rotation speed of the sample holder controlled the thickness of the prepared Mo films. Next, the pre-deposited Mo layers were sulfurized in a custom-designed CVD chamber. The Mo layer was annealed in sulfur vapors at a high temperature of 800 °C in an N_2 atmosphere at ambient pressure. The substrate was placed together with the sulfur powder in the center of the furnace so that the temperature of the substrate and the powder were the same during the growth, unlike the standard CVD method, which uses a two-zone furnace with different temperatures for the sulfur powder and the Mo substrate [14].

2.3 GOs

GO was prepared using a modified Hummers method from graphite powder. rGO was made from GO dispersion, evaporating in a water bath to yield a mud-like residue. The sample was treated in ascorbic acid solution and sonicated. SH-GO arose from GO. GO was refluxed and stirred in a toluene/P_4S_{10} solution for 7 days. All active layers were prepared by drop-casting of 20 µl acetone suspension (ratio of 1 g in 25 ml).

2.4 Au NPs

The Au NPs were prepared by evaporating a thin Au layer (thickness of about 3 nm), which was further annealed in hydrogen microwave plasma. This treatment resulted in the formation of nano-sized Au particles (droplets) on the H-NCD surface. The Au was chosen due to its chemical stability and simple preparation [15].

2.5 Heterostructures

The preparation of heterostructures combined previous technological steps to prepare active layers for gas sensors. The first layer is, in most cases, H-NCD and the second material is prepared on it. The prepared heterostructures were kept for a week to stabilize the sensor surface [14,15].

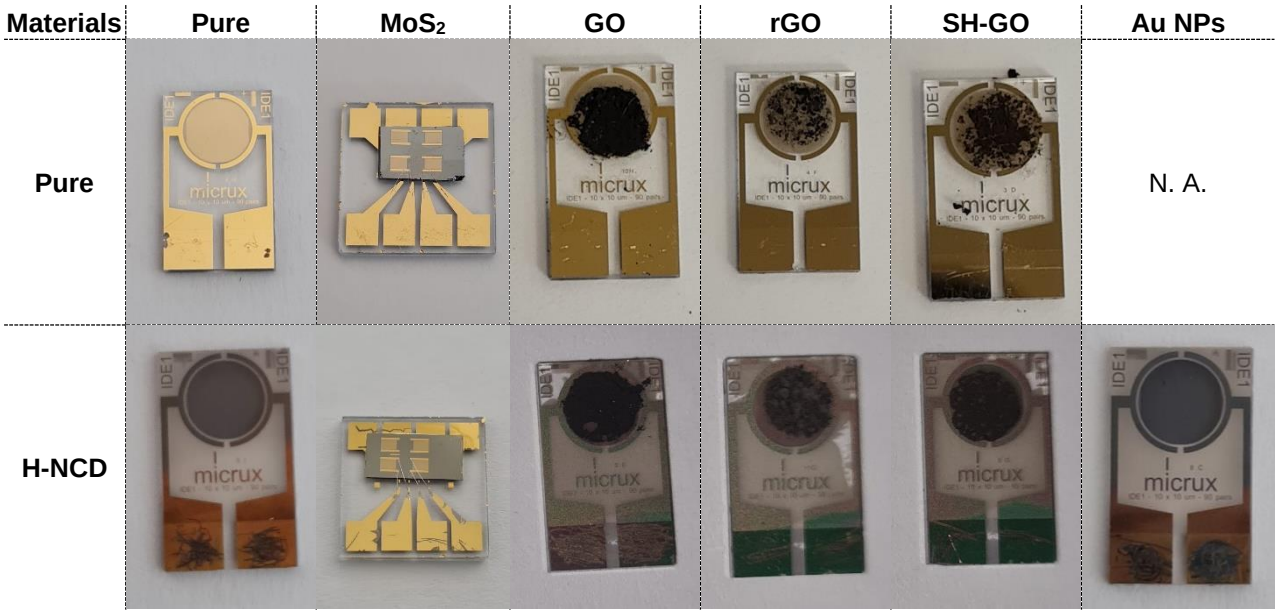

Figure 1 Photographs of all fabricated and tested sensors with pure materials and heterostructures

3. RESULTS AND DISCUSSION

The gas responses of these sensors were measured at a high temperature of 125 °C and room temperature (about 22 °C) for three testing gases concentrated at 100 ppm: ethanol vapor, NH_3, and NO_2. The gas-sensitive layer changed the resistance from steady-state R_0 to actual resistance R_G in the presence of the tested gas. The resistance changes Δ_R in the presence of active gas were calculated using equation (1). **Table 1** and **Table 2** show the responses achieved for individual sensors.

$$\Delta_R = \left(\frac{R_G}{R_0} - 1\right) \cdot 100 = \left(\frac{R_G - R_0}{R_0}\right) \cdot 100\ (\%) \quad (1)$$

Where:

Δ_R – Resistance change (%)

R_G – Resistance in the presence of the tested gas (Ω)

R_0 – Steady-state resistance (Ω)

Table 1 Responses of sensors at 125 °C exposed to 100 ppm ethanol vapor, 100 ppm NH_3 and 100 ppm NO_2. In the table, the best and the second-best values are highlighted in dark green and light green.

125 °C	Pure			H-NCD		
	100 ppm Ethanol	100 ppm NH_3	100 ppm NO_2	100 ppm Ethanol	100 ppm NH_3	100 ppm NO_2
Pure [13]	No response			98	39	-13
MoS_2	Unmeasured					

GO	352	28	-39	498	69	-40
rGO	148	-11	17	254	72	-39
SH-GO	46	8	-5	554	76	-47
Au NPs [15]	Unmeasured			587	48	-47

Table 2 Responses of sensors at 22 °C exposed to 100 ppm ethanol vapor, 100 ppm NH_3 and 100 ppm NO_2. In the table, the best and the second-best values are highlighted in dark green and light green.

RT (22 °C)	Pure			H-NCD		
	100 ppm Ethanol	100 ppm NH_3	100 ppm NO_2	100 ppm Ethanol	100 ppm NH_3	100 ppm NO_2
Pure [13]	No response			3	0.5	-0.7
MoS_2 [14]	35	-0.7	1.8	248	17.8	15.7
GO	301	5.2	-7.9	153	2.1	-7.2
rGO	130	-2	1.8	195	7.1	-2.2
SH-GO	16	0.6	-0.2	634	41	-19
Au NPs [15]	Unmeasured			164	4.8	-4.7

The responses are summarized and compared in **Figures 2**, **3**, and **4**. Compared to pure materials, their combination in heterostructure significantly enhanced the gas responses. The best response to gases exhibited SH-GO/H-NCD and Au NPs/H-NCD heterostructures at 125 °C, respectively SH-GO/H-NCD at room temperature. The SH-GO/H-NCD sensor exposed to 100 ppm ethanol achieved the most significant response of 634 % and 554 % at 22 °C and 125 °C, respectively. The second-best ethanol sensor is a heterostructure of Au NPs/H-NCD with a response of 587 % at 125 °C. The pure materials revealed a low response (<2 %) at room temperature, except for GO, with very high steady-state resistance. The higher temperature enhanced the response of almost all sensors. The only exception is the ethanol response of SH-GO/H-NCD. In this case, the response decreased from 634 % to 554 %.

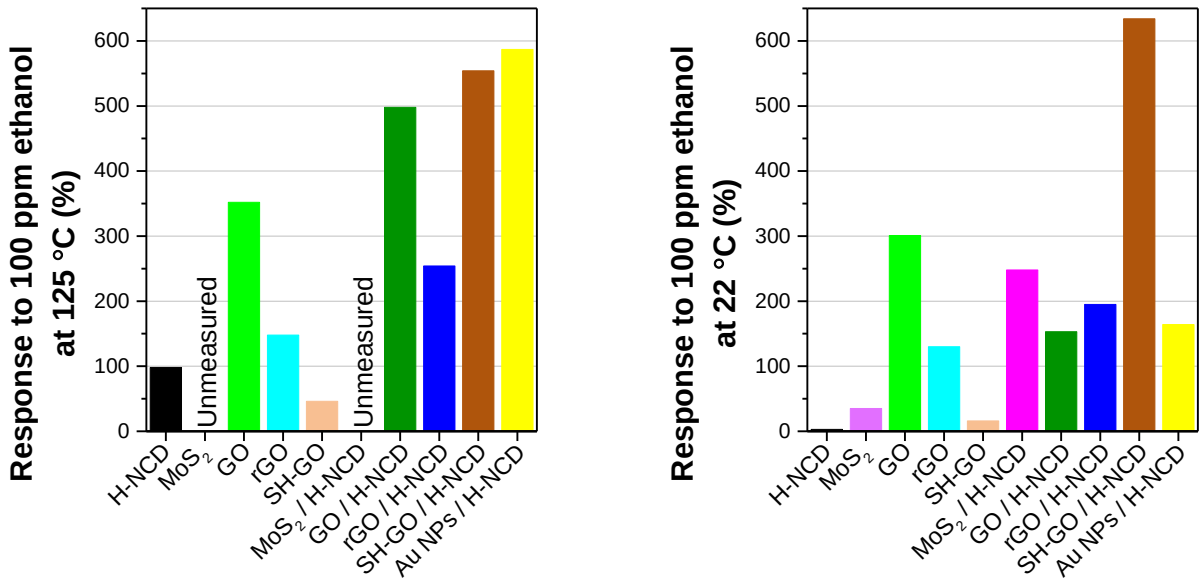

Figure 2 Responses of fabricated sensors to 100 ppm ethanol vapor at 125 °C and 22 °C (room temperature)

In comparison with commercial gas sensors, our sensors achieved comparable responses. For example, the commercially available conductivity sensor TGS 826 from Figaro is designed to detect NH_3 with a concentration from 30 ppm to 300 ppm [16]. This sensor uses SnO_2 as active material heated to 300 °C. The measured response to NH_3 is -16.9 % and 47.8 % to NO_2 [13]. A similar response to NO_2 had an IR gas sensor PY2055 from Pyreos, which is designed to detect NO_2 [17]. This sensor uses the absorption of IR light by gas. The disadvantage is the need to use an IR light source and as long as possible interaction path where the light will be absorbed. The total response to NO_2 is -46 %. This sensor had no response to NH_3, because this type has very high selectivity [13]. All prepared heterostructures have comparable responses at 125 °C to gases with these commercial sensors. In addition, the SH-GO/H-NCD and MoS_2/H-NCD have good responses comparable with commercial sensors at room temperature.

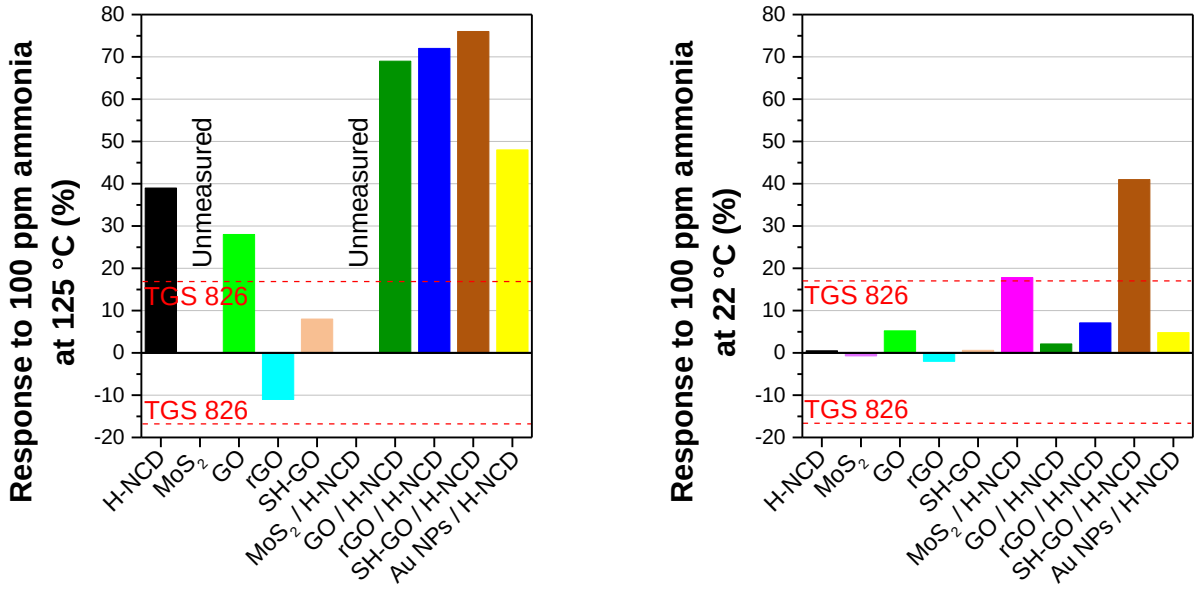

Figure 3 Responses of fabricated sensors to 100 ppm NH_3 at 125 °C and 22 °C (room temperature)

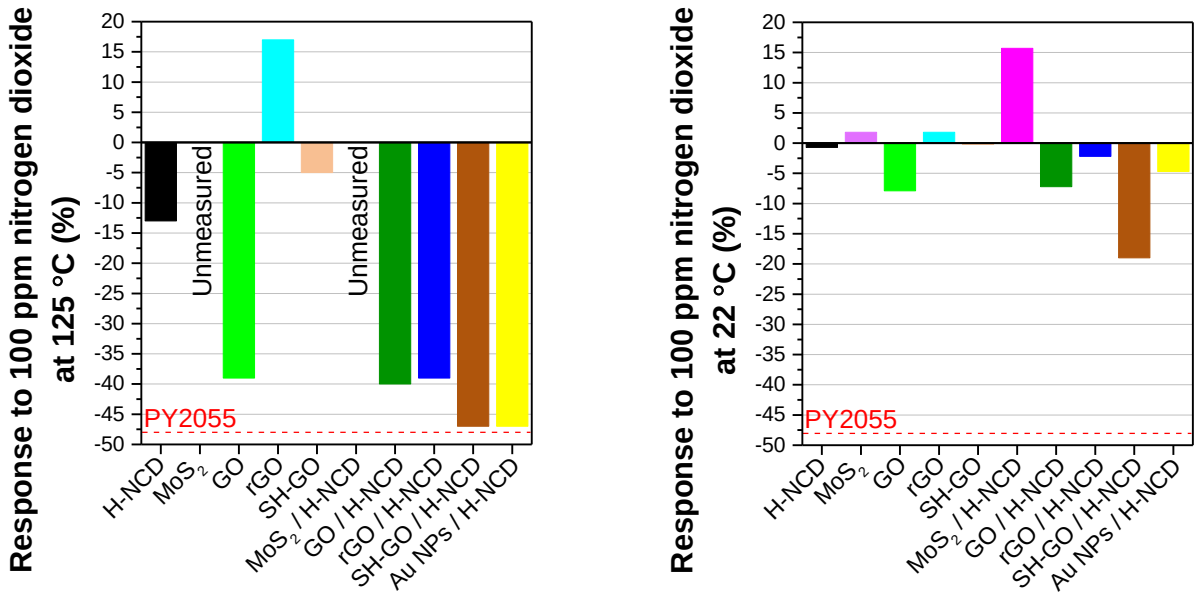

Figure 4 Responses of measured sensors to 100 ppm NO_2 at 125 °C and 22 °C (room temperature)

4. CONCLUSION

The newly introduced heterostructures H-NCD and the second material (MoS_2, GO, rGO, SH-GO or Au NPs) were designed, fabricated, and tested. The measurements revealed that most heterostructures exhibit preferable responses to exposed gas compared with pure materials at high and room temperatures. Even, the responses of some heterostructures are comparable with commercial gas sensors at 22 °C.

At a high temperature of 125 °C, all heterostructures and pure materials respond very well. At these conditions, the best responses exhibited SH-GO/H-NCD and Au NPs/H-NCD heterostructures with responses over 47 % for all tested gases, which are well comparable with commercial sensors. The power consumption for our heater should be still optimized, but it is much lower than the power needed for commercial sensors. For room temperature applications, pure materials and some heterostructures have very low, almost immeasurable, responses. The best combination of materials with good responses is SH-GO/H-NCD and MoS_2/H-NCD. These sensors have a response of over 15 % for all tested gases. These high responses are attributed to the optimum steady-state resistance, further enhanced by the synergistic effect at the interface of active materials.

In conclusion, our findings represent a promising alternative solution as the new class of gas sensors suitable for portable or energy-harvesting applications due to miniaturization and low power consumption. For now, however, the reproducibility of sensor production technology needs to be scaled up and optimized to meet industrial uses.

ACKNOWLEDGEMENTS

This research was funded by the mobility projects CSIR-23-05 and PAN 20 21 of the Czech Academy of Sciences. This work used the research infrastructure CzechNanoLab supported by the LM2023051 project and partially by CTU University project No. SGS23/181/OHK3/3T/13 Materials and structures for sensors, integrated and photonic circuits.

REFERENCES

[1] FRADEN, J. *Handbook of modern sensors: Physics, designs, and applications*, 3rd ed. New York: Springer. 2003. ISBN: 0-387-00750-4.

[2] DHALL, S., MEHTA, B. R., TYAGI, A. K., SOOD, K. A review on environmental gas sensors: Materials and technologies. *Sensors International*. 2021, vol. 2, 100116. Available from: https://doi.org/10.1016/j.sintl.2021.100116

[3] ŠTULÍK, K., BAREK, J., JANATA, J., KRÁL, V., KRONĎÁK, M., ŠŤASTNÝ, M. *SENZORY: General Aspects of Chemical Sensing*. VŠCHT Praha, 2007, ISBN: 978-80-86238-20-3.

[4] WANG, C., YIN, L., ZHANG, L., XIAND, D., GAO, R. Metal Oxide Gas Sensors: Sensitivity and Influencing Factors. *Sensors*. 2010. Available from: https://doi.org/10.3390/s100302088.

[5] HELWIG, A., MUELLER, G., GARRIDO, J. A., EICKHOFF, M. Gas sensing properties of hydrogen-terminated diamond. *Sensors and Actuators B: Chemical*. 2008. Available from: https://doi.org/10.1016/j.snb.2008.02.007.

[6] GURBUZ, Y., KANG, W. P., DAVIDSON, J. L., KINSER, D. L., KERNS, D.V. Diamond microelectronic gas sensors. *Sensors and Actuators B: Chemical*. 1996. Available from: https://doi.org/10.1016/0925-4005(96)01839-4.

[7] MÜELLER, G., KRSTEV, I., MAIER, K., HELWIG, A., STUTZMANN, M., GARRIDO, J. Resettable, low-temperature accumulation gas sensors based on hydrogenated diamond transducers. *EUROSENSORS 2015*. 2015. Available from: https://doi.org/10.1016/j.proeng.2015.08.733.

[8] NEETIKA, KUMAR, A., CHANDRA, R., MALIK, V. K. MoS2 nanoworm thin films for NO2 gas sensing application. *Thin Solid Films*. 2021. Available from: https://doi.org/10.1016/j.tsf.2021.138625.

[9] LUO, H., CAO, Y., ZHOU, J., FENG, J., CAO, J., GUO, H. Adsorption of NO2, NH3 on monolayer MoS2 doped with Al, Si, and P: A first-principles study. *Chemical Physics Letters*. 2016. Available from: https://doi.org/10.1016/j.cplett.2015.10.077.

[10] SHOKRI, A., SALAMI, N. Gas sensor based on MoS2 monolayer. *Sensors and Actuators B: Chemical*. 2016. Available from: https://doi.org/10.1016/j.snb.2016.06.033.

[11] KUMAR, R., AVASTHI, D. K., KAUR, A. Fabrication of chemoresistive gas sensors based on multistep reduced graphene oxide for low parts per million monitoring of sulfur dioxide at room temperature. *Sensors and Actuators B: Chemical*. 2017. Available from: https://doi.org/10.1016/j.snb.2016.11.018.

[12] DING, L., QIN, Z., DOU, Z., SHEN, Y., CAI, Y., ZHANG, Y., ZHOU, Y. Morphology-promoted synergistic effects on the sensing properties of polyaniline ultrathin layers on reduced graphene oxide sheets for ammonia and formaldehyde detection. *J Mater Sci*. 2018. Available from: https://doi.org/10.1007/s10853-018-2109-7.

[13] KOČÍ, M., KROMKA, A., BOUŘA, A., SZABÓ, O., HUSÁK, M. Hydrogen-Terminated Diamond Surface as a Gas Sensor: A Comparative Study of Its Sensitivities. Sensors (Basel, Switzerland). 2021, vol. 21, no. 16. Available from: https://doi.org/10.3390/s21165390.

[14] KOČÍ, M., IZSÁK, T., VANKO, G., SOJKOVÁ, M., HRDÁ, J., SZABÓ, O., HUSÁK, M., VÉGSÖ, K., VARGA, M., KROMKA, A. Improved Gas Sensing Capabilities of MoS2/Diamond Heterostructures at Room Temperature. *ACS applied materials & interfaces*. 2023. Available from: https://doi.org/10.1021/acsami.3c04438.

[15] KOČÍ, M., SZABÓ, O., VANKO, G., HUSÁK, M., KROMKA, A. Enhanced gas sensing capabilities of diamond layers using Au nanoparticles. *Diamond and Related Materials*. 2023. Available from: https://doi.org/10.1016/j.diamond.2023.110218.

[16] FIGARO USA, INC. *TGS 826 - for the Detection of Ammonia: Product Information*. Available online: https://www.figarosensor.com/product/docs/TGS%20826%20%2805_04%29.pdf.

[17] Pyreos Limited. *Thin Film Pyroelectric Dual Channel Sensor: Product Information*. Available online: https://pyreos.com/wp-content/uploads/2020/11/Pyreos-Analog-TO-Two-Channels.pdf